ISSN 0036-0236, Russian Journal of Inorganic Chemistry, 2017, Vol. 62, No. 6, pp. 736–745. © Pleiades Publishing, Ltd., 2017.
Original Russian Text © R.E. Khoma, V.O. Gel'mbol'dt, A.A. Ennan, V.N. Baumer, A.N. Puzan, T.V. Koksharova, A.V. Mazepa, 2017, published in Zhurnal Neorganicheskoi Khimii, 2017, Vol. 62, No. 6, pp. 751–760.

COORDINATION COMPOUNDS

Onium Salts of Sulfur-Containing Oxyanions Resulting from Reaction of Sulfur(IV) Oxide with Aqueous Solutions of 1,2-Diamines and Morpholine

R. E. Khoma[a, b, *], V. O. Gel'mbol'dt[c], A. A. Ennan[a], V. N. Baumer[d], A. N. Puzan[d], T. V. Koksharova[b], and A. V. Mazepa[e]

[a] *Physicochemical Institute for Environment and Human Protection, National Academy of Sciences of Ukraine, Odessa, 65082 Ukraine*
[b] *Odessa National University, Odessa, 65082 Ukraine*
[c] *Odessa National Medical University, Odessa, 65082 Ukraine*
[d] *Institute of Single Crystals, National Academy of Sciences of Ukraine, Kharkov, 61001 Ukraine*
[e] *Bogatskii Physicochemical Institute, National Academy of Sciences of Ukraine, Odessa, 65080 Ukraine*
**e-mail: rek@onu.edu.ua*

Received July 14, 2016

Abstract—Reaction products have been isolated from SO_2–L–H_2O–O_2 systems (L = ethylenediamine, *N*,*N*,*N*',*N*'-tetramethylethylenediamine, piperazine, and morpholine) as onium salts $[H_3NCH_2CH_2NH_3]SO_4$, $[(CH_3)_2NHCH_2CH_2NH(CH_3)_2]SO_4$, $[(CH_3)_2NHCH_2CH_2NH(CH_3)_2]S_2O_6 \cdot H_2O$, $[C_4H_8N_2H_4]SO_3 \cdot H_2O$, $[C_4H_8N_2H_4]S_2O_6$, $[C_4H_8N_2H_4]SO_4 \cdot H_2O$, $[O(C_2H_4)_2NH_2]_2SO_4 \cdot H_2O$. The prepared compounds have been characterized by X-ray diffraction analysis, X-ray powder diffraction, IR and mass spectroscopy.

DOI: 10.1134/S0036023617060109

Ethylenediamine (EDA), *N*,*N*,*N*',*N*'-tetramethylethylenediamine (TMEDA), piperazine (PP), and its structural analog morpholine (MP) exhibit properties of mono- and diacidic bases producing salts with mineral and organic acids [1–8]. The interest in this group of compounds is associated with the possibility of their practical application.

In particular, ethylenediammonium salts are promising materials for nonlinear optics [3], they show proton and dielectric conductance [4]. Ethylenediammonium dicarboxylates exhibit antimicrobial and fungicide activity [8], PP and its salts are used in medicine and veterinary as anthelmintic remedies [1]. In this paper, we describe method of synthesis, structural study, spectral properties, and thermal stability of products resulting from the reaction of SO_2 with aqueous solutions of 1,2-diamines and morpholine in the presence of air oxygen.

EXPERIMENTAL

Ethylenediammonium sulfate (I). A solution of EDA monohydrate (0.10 mol) in 10 mL of water was placed into a thermostatted cell, gaseous SO_2 was bubbled through the solution at 0°C at a rate 50 mL/min until pH < 1.0. The solution with precipitate was subjected to isothermal evaporation at ambient temperature in air until complete removal of water. The isolated white crystalline product I (15.61 g, yield toward EDA 98.7%; mp 225–227°C) was used without additional purification.

MS: $[SO_2]^+$ ($m/z = 64$, $I = 42\%$); $[M_L]^+$ ($m/z = 60$, $I = 5\%$); $[M_L–H]^+$ ($m/z = 59$, $I = 5\%$); $[SO]^+$ ($m/z = 48$, $I = 19\%$); $[CH_3CH{=}NH_2]^+$ ($m/z = 44$, $I = 5\%$); $m/z = 43$, $I = 10\%$; $m/z = 42$, $I = 8\%$; $[CH_2{=}NH_2]^+$ ($m/z = 30$, $I = 100\%$).

For $C_2H_{10}N_2O_4S$ anal. calcd. (%): C, 15.19; H, 6.37; N, 17.71; S, 20.27. *M* 158.18. Found (%): C, 15.07; H, 6.23; N, 17.12; S, 20.64.

A mixture of *N*,*N*,*N*',*N*'-tetramethylethylenediammonium sulfate dihydrate (IIa) and *N*,*N*,*N*',*N*'-tetramethylethylenediammonium dithionate monohydrate (IIb). Similar procedure for a TMEDA aqueous solution (0.05 mol of the amine in 10 mL of H_2O) gave rise to 6.43 g of a yellow–brown mixture of crystalline products **IIa** and **IIb**.

Anal. calcd. (%): C, 25.62; H, 7.88; N, 9.96; S, 16.91. Found (%): C, 25.74; H, 7.97; N, 9.88; S, 16.85.

A mixture of piperazinium sulfite (IIIa), piperazinium dithionate (IIIb), and piperazinium sulfate monohydrate (IIIc). Similar procedure for an aqueous solu-

tion of PP octahydrate (0.05 mol of the amine in 10 mL of H_2O) resulted in 10.66 g of a white mixture of crystalline products **IIIa**, **IIIb**, and **IIIc**.

MS: $[M_L]^+$ ($m/z = 86$, $I = 34\%$); $[M_L-H]^+$ ($m/z = 85$, $I = 28\%$); $m/z = 80$, $I = 28\%$; $[SO_2]^+$ ($m/z = 64$, $I = 24\%$); $[CH_2CH_2NH{=}CH_2]^+$ ($m/z = 57$, $I = 30\%$); $[CH_2{=}CHNH{=}CH_2]^+$ ($m/z = 56$, $I = 31\%$); $[SO]^+$ ($m/z = 48$, $I = 17\%$); $[CH_2{=}NHCH_3]^+$ ($m/z = 44$, $I = 100\%$); $[CH_2{=}NH_2]^+$ ($m/z = 30$, $I = 31\%$).

Anal. calcd. (%): C, 24.90; H, 7.24; N, 14.51; S, 17.75. Found (%): C, 24.98; H, 7.38; N, 14.43; S, 17.67.

Morpholinium sulfate monohydrate (IV). Similar procedure for an aqueous solution of MP (0.10 mol of the amine in 10 mL of H_2O) resulted in 12.62 g of white crystalline product **IV** (yield 87.0% toward MP, mp 20–22°C).

MS: $[M_L]^+$ ($m/z = 87$, $I = 66\%$); $[M_L-H]^+$ ($m/z = 86$, $I = 27\%$); $[SO_2]^+$ ($m/z = 64$, $I = 27\%$); $[M_L-CH_2O]^+$ ($m/z = 57$, $I = 100\%$); $[M_L-CH_2O-H]^+$ ($m/z = 56$, $I = 35\%$); $[SO]^+$ ($m/z = 48$, $I = 32\%$); $[CH_2{=}NH_2]^+$ ($m/z = 30$, $I = 41\%$).

For $C_8H_{22}N_2O_7S$ anal. calcd. (%): C, 33.10; H, 7.64; N, 9.65; S, 38.57; *M* 290.34. Found (%): C, 29.76; H, 7.51; N, 9.53; S, 39.03.

Analysis for carbon, hydrogen, and nitrogen content was carried out on a CHN analyzer, sulfur was determined by the Schoniger technique [9]. X-ray diffraction study of compounds II–IV was performed on an Oxford Diffraction Xcalibur-3 diffractometer (MoK_α radiation, graphite monochromator, Sapphire-3 CCD detector). The structure was solved and refined using SHELX-97 software package [10]. Hydrogen atoms were located from a difference-Fourier map and refined using the Riding model for methyl and methylene groups. Hydrogen atoms involved in hydrogen bonding (HB) were refined in isotropic approximation. X-ray powder diffraction (XRD) was accomplished on a Siemens D500 powder diffractometer (Bragg–Bretano geometry, CuK_α radiation, Ni filter). IR spectra were recorded on a Perkin-Elmer Spectrum BX II FT-IR System spectrophotometer in 4000–350 cm^{-1} region as KBr pellets, mass spectra were obtained on a MX-1321 instrument (direct inlet into source, ionizing voltage 70 eV).

The main crystallographic data and refinement results for structures **IIa**–**IV** are presented in Table 1. Atom coordinates, structural factors and all refinement results were deposited in the Cambridge Crystallographic Data Center (Table 1). Geometrical characteristics of hydrogen bonds observed in structures **IIb**–**IV** are given in Table 2.

RESULTS AND DISCUSSION

The mass spectrum of compound I displays fragmentation typical for 1-*n*-alkylamines [11] resulting in formation of $[CH_2{=}NH_2]^+$ ion with peak of the maximal intensity. Piperazine fragmentation products in the mass spectrum of mixture of its onium salts **IIIa**, **IIIb**, and **IIIc** agree well with the tabulated mass spectrum of PP [11]. Similar agreement is observed for MP.

According to X-ray diffraction study, compound **I** is ethylenediammonium sulfate structurally characterized previously [2]. TMEDA produces a mixture of onium sulfate **IIa** and dithionate dihydrate IIb. Structure **IIa** was also described in the literature [12] and is not discussed below. In structure **IIb** (Fig. 1), cation and anion occupy the centers of symmetry while water molecule is in a general position. Bond distances and valence angles have common values for similar compounds. Packing in crystal causes formation of 2D system of hydrogen bonds (Table 2) producing layers in (001) planes. Rietveld refinement for powder diffraction patterns of reaction product showed almost equal content of compounds **IIa** and **IIb** in powder (**IIa** : **IIb** = 46 : 54).

The reaction of SO_2 with aqueous solution of PP leads to formation of three compounds: sulfite monohydrate **IIIa**, dithionate **IIIb**, and sulfate monohydrate **IIIc**. The structure of compound **IIIa** (Fig 2) includes both cations in the centers of symmetry. Bond distances and valence angles are common. The compound forms a 3D system of hydrogen bonds in crystal (Table 2). Both basis molecules in structure **IIIb** (Fig. 3) are in general position. Dithionate ions in crystal are located in (100) coordinate planes, cation layers are located between them. A branched 3D system of hydrogen bonds is formed in the structure (Table 2). Structure **IIIc** includes two cations located in the centers of symmetry (Fig. 4). Crystal contains cation layers in (001) planes, while anions and water molecules are located in cavities between the layers. The system of hydrogen bonds in structure **IIIc** is three-dimensional. To determine compound ratio in reaction product, we calculated powder diffractogram of the latter by the Rietveld method using found by us structure models **IIIa**, **IIIb**, and **IIIc** (Fig. 5). The found composition is as follows (wt %): **IIIa**, 74.8; **IIIb**, 8.8; **IIIc**, 16.4. Figure 5 shows that the reaction product contains no other substances.

The reaction of SO_2 with aqueous solution of MP leads to only one compound, morpholinium (IV) sulfate monohydrate, whose structure is shown in Fig. 6. Like in compound **IIIc**, the structure **IV** includes anions and water molecules between cation layers producing a 3D system of hydrogen bonds.

The data of IR spectroscopy (Table 3) indicate that reaction product of PP contains sulfite ion, whereas other obtained products contain sulfate ions. The IR spectra of products obtained from TMEDA and PP exhibit also absorption bands of dithionate anions.

Table 1. Crystallographic data, X-ray diffraction conditions, and structure refinement characteristics for **IIb**, **IIIa**, **IIIb**, **IIIc**, and **IV**

Characteristic	**IIa**	**IIb**	**IIIa**	**IIIb**	**IIIc**	**IV**
Molecular formula	$C_6H_{22}N_2O_6S$	$C_6H_{22}N_2O_8S_2$	$C_4H_{14}N_2O_4S$	$C_4H_{12}N_2O_6S_2$	$C_4H_{14}N_2O_5S$	$C_8H_{22}N_2O_7S$
CCDC code	CCDC 1481226	CCDC 1481220	CCDC 1481221	CCDC 1481222	CCDC 1481223	CCDC 1481224
FW	250.32	314.38	186.23	248.28	202.23	290.34
Syngony	Monoclinic	Triclinic	Monoclinic	Triclinic	Monoclinic	Rhombic
T, K	293(2)	293(2)	293(2)	293(2)	293(2)	110(2)
Space group	$P2_1/n$	$P\bar{1}$	$P2_1/c$	$P\bar{1}$	$P2_1/n$	$P2_12_12_1$
a, Å	8.4127(7)	7.1407(2)	11.8095(5)	6.6132(6)	6.3701(4)	6.4381(3)
b, Å	9.4782(12)	7.2243(3)	6.4251(2)	6.7771(6)	11.6392(6)	13.2098(6)
c, Å	15.2659(14)	8.2808(2)	10.7396(5)	10.1445(11)	11.6572(6)	14.9798(7)
α, deg	90	105.939(3)	90	94.866(8)	90	90
β, deg	93.046(9)	109.674(3)	92.616(4)	94.907(8)	101.034(5)	90
γ, deg	90	105.041(3)	90	95.789(8)	90	90
V, Å^3	1215.5(2)	356.36(2)	814.04(6)	448.68(7)	848.32(8)	1273.97(10)
Z	4	1	4	2	4	4
ρ, g/cm^3	1.368	1.465	1.520	1.838	1.583	1.514
μ(MoK_α), mm^{-1}	0.279	0.406	0.371	0.603	0.372	0.284
θ range, deg	3.24–26.00	3.18–29.98	3.61–30.00	5.72–26.00	3.40–32.24	3.08–25.99
Crystal dimensions, mm	0.20 × 0.06 × 0.05	0.20 × 0.05 × 0.04	0.25 × 0.15 × 0.10	0.5 × 0.3 × 0.2	0.22 × 0.14 × 0.03	0.20 × 0.15 × 0.05
F_{000}	544	168	400	260	432	624
T_{min}/T_{max}	0.946/0.986	0.923/0.984	0.913/0.964	0.753/0.889	0.923/0.989	0.945/0.986
Number of reflections: measured	4321	3373	7510	2467	4526	8258
independent with $I_{hkl} > 2\sigma(I)$	2174	2026	2335	1599	2628	2440
R_{int}	0.0315	0.0343	0.0310	0.0254	0.0249	0.0387
Fullness, %	91.2	97.7	98.6	95.3	98.1	97.6
Number of refined parameters	160	97	158	123	129	231
R_F/wR^2 on observed reflections	0.0482/0.1138	0.0363/0.0737	0.0320/0.0860	0.0520/0.1395	0.0371/0.0747	0.0294/0.0584
R_F/wR^2 on independent reflections	0.0710/0.1240	0.0479/0.0784	0.0397/0.0905	0.0638/0.1521	0.0581/0.0808	0.0355/0.0605
S	0.967	0.992	0.986	0.987	0.968	0.931
$\Delta\rho_{min}/\Delta\rho_{max}$, e/Å^3	–0.289/0.491	–0.352/0.238	–0.424/0.415	–0.415/0.485	–0.264/0.270	–0.240/0.163

Table 2. Geometrical characteristics of hydrogen bonds in structures IIb, IIIa, IIIb, IIIc, and IV

Contact D–H···A	Distance, Å			DHA angle, deg	Transformation for atom A
	d(D–H)	*d*(H···A)	*d*(D···A)		
IIb					
N(1)–H(1)···O(4)	0.819(14)	1.983(14)	2.7614(14)	158.5(12)	
N(1)–H(1)···O(3)	0.819(14)	2.654(12)	3.1033(12)	116.1(11)	$x + 1, y, z$
O(4)–H(4A)···O(2)	0.850(18)	1.927(18)	2.7645(13)	168.4(13)	
O(4)–H(4B)···O(1)	0.804(15)	2.050(15)	2.8520(12)	174.9(17)	$-x + 2, -y + 2, -z + 1$
IIIa					
O(4)–H(4A)···O(3)	0.86(2)	2.00(2)	2.8513(16)	178(2)	$x, y - 1, z$
O(4)–H(4B)···O(2)	0.78(2)	2.05(2)	2.8174(16)	167(2)	
N(1)–H(1A)···O(1)	0.881(15)	1.870(16)	2.7309(13)	165.0(14)	
N(1)–H(1B)···O(1)	0.859(17)	1.852(17)	2.7096(13)	175.7(15)	$-x + 1, y + 1/2, -z + 3/2$
N(2)–H(2A)···O(3)	0.870(16)	1.844(17)	2.7037(14)	169.1(16)	$-x + 1, -y, -z + 1$
N(2)–H(2B)···O(2)	0.929(18)	1.805(18)	2.6831(13)	156.6(16)	$-x + 1, y + 1/2, -z + 3/2$
IIIb					
N(1)–H(1A)···O(4)	0.75	2.00	2.748(3)	171.3	$x + 1, y, z$
N(1)–H(1B)···O(6)	0.75	2.08	2.811(3)	167.0	$x + 1, y - 1, z$
N(2)–H(2A)···O(3)	0.74	2.07	2.796(3)	165.7	
N(2)–H(2B)···O(1)	0.74	2.04	2.758(3)	164.6	$x, y - 1, z$
IIIc					
O(5)–H(5A)···O(4)	0.81(2)	2.09(2)	2.878(2)	165(2)	$x + 1, y, z$
O(5)–H(5B)···O(2)	0.77(2)	2.04(2)	2.8140(19)	176(2)	
N(1)–H(1A)···O(1)	0.92(2)	1.84(2)	2.7576(16)	170.5(18)	$x + 1/2, -y + 1/2, z + 1/2$
N(1)–H(1B)···O(3)	0.88(2)	1.92(2)	2.7810(18)	169.5(19)	$-x + 1, y + 1/2, -z + 3/2$
N(2)–H(2A)···O(1)	0.897(19)	1.899(19)	2.7711(15)	163.5(19)	$-x + 1, y + 1/2, -z + 3/2$
N(2)–H(2B)···O(3)	0.89(2)	1.86(2)	2.7387(16)	170.7(18)	
IV					
O(7)–H(7B)···O(5)#1	0.76(2)	1.95(2)	2.7155(17)	175(2)	$x - 1, y, z$
O(7)–H(7A)···O(6)	0.836(19)	1.94(2)	2.7664(17)	168.7(19)	
N(1)–H(1A)···O(3)	0.882(18)	1.960(18)	2.8199(19)	164.6(17)	
N(1)–H(1B)···O(6)#2	0.896(19)	1.973(19)	2.844(2)	163.8(18)	$-x + 2, y + 1/2, -z + 3/2$
N(1)–H(1B)···O(5)#2	0.896(19)	2.652(19)	3.1863(19)	119.2(14)	$-x + 2, y + 1/2, -z + 3/2$
N(2)–H(2B)···O(4)#2	0.881(19)	1.829(19)	2.7102(19)	178.0(18)	$-x + 2, y + 1/2, -z + 3/2$
N(2)–H(2A)···O(7)#3	0.89(2)	1.87(2)	2.758(2)	173.9(17)	$x + 1/2, -y + 1/2, -z + 1$

The assignment of bands in IR spectra was made taking into account the literature data [5–7, 13–15].

Free pyramidal SO_3^{2-} ion is known [15] to be related to C_{3v} point group and has four main vibration frequencies: $\nu_1(A_1) = 967$, $\nu_2(A_1) = 620$, $\nu_3(E) = 933$; and $\nu_4(E) = 469$ cm^{-1}.

The IR spectrum of the mixture of compounds **IIIa**, **IIIb**, and **IIIc** show stretching vibrations ν(SO) of SO_3^{2-} ion (ν_1 and ν_3, respectively) as strong absorption bands at 952 and 905 cm^{-1}. This region also includes weaker bands at 1029, 1008, and 992 cm^{-1}. Two bands—medium intensity band at 492 cm^{-1} and a shoulder at 572 cm^{-1}—can be considered as a result of splitting of doubly degenerated out-of-plane deformational vibration $\nu_4(E)$ of ion $S_2O_6^{2-}$. Symmetrical deformational vibration $\delta_s(SO_3^{2-})$ (ν_2) of SO_3^{2-} ion appears as a medium intensity band at 620 cm^{-1}.

Absorption bands with maxima at 3384 and 3247 cm^{-1} are related to asymmetrical and symmetrical ν(N–H) stretching vibrations, whereas lower frequency strong band at 3020 cm^{-1} can be assumingly assigned to vibrations with preferable contribution of ν(N^+H).

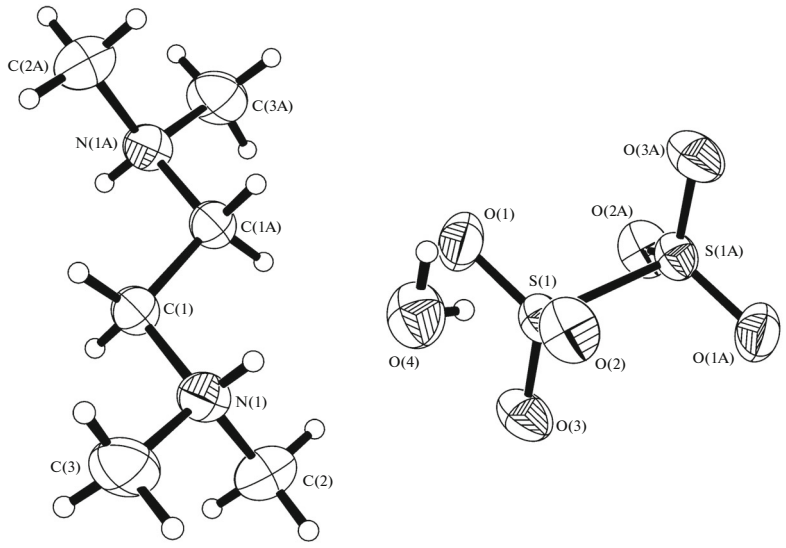

Fig. 1. Atom numbering scheme and thermal ellipsoids (probability level 50%) for structure **IIb**. Letter A marks symmetrically equivalent atoms.

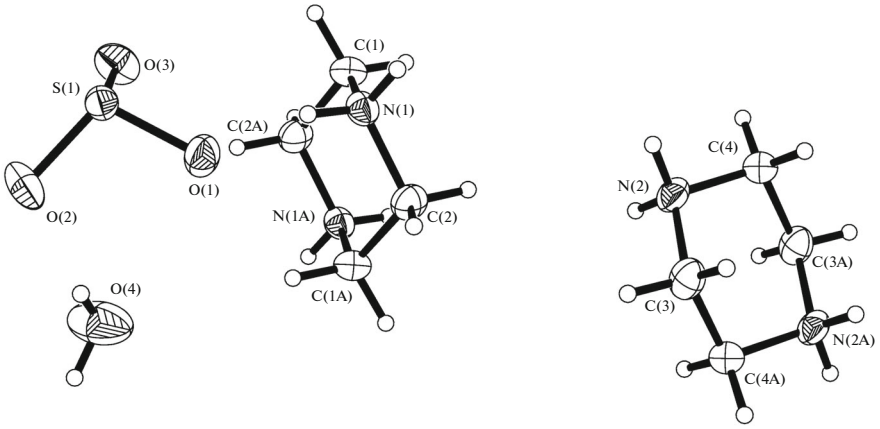

Fig. 2. Atom numbering scheme and thermal ellipsoids (probability level 50%) for structure **IIIa**. Letter A marks symmetrically equivalent atoms.

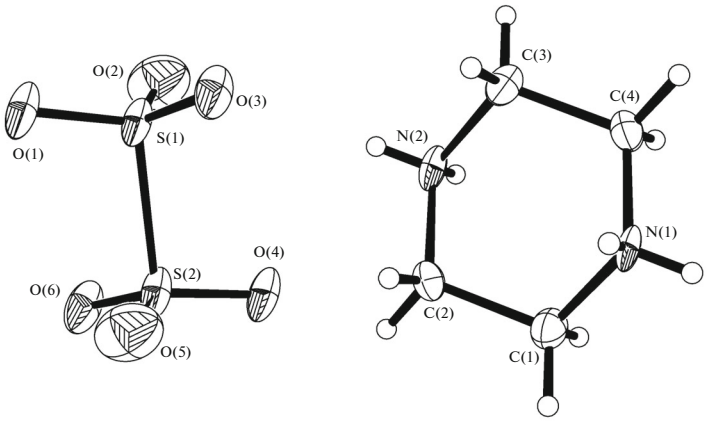

Fig. 3. Atom numbering scheme and thermal ellipsoids (probability level 50%) for structure **IIIb**.

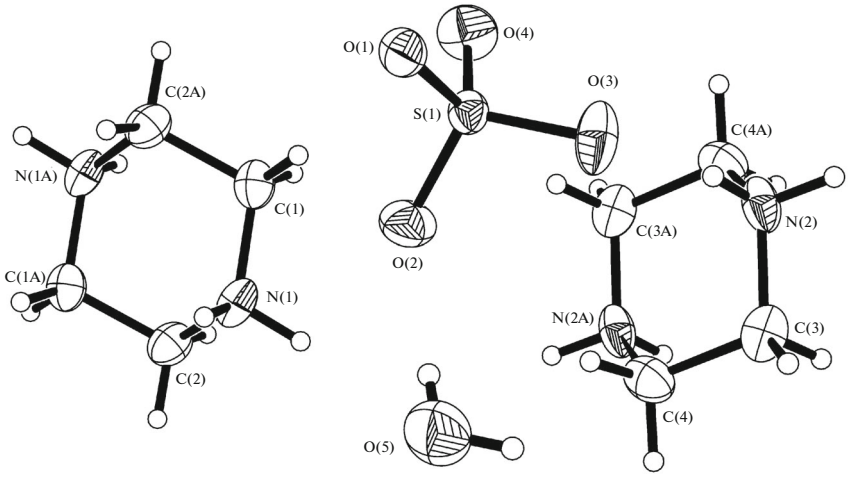

Fig. 4. Atom numbering scheme and thermal ellipsoids (probability level 50%) for structure **IIIc**. Letter A marks symmetrically equivalent atoms.

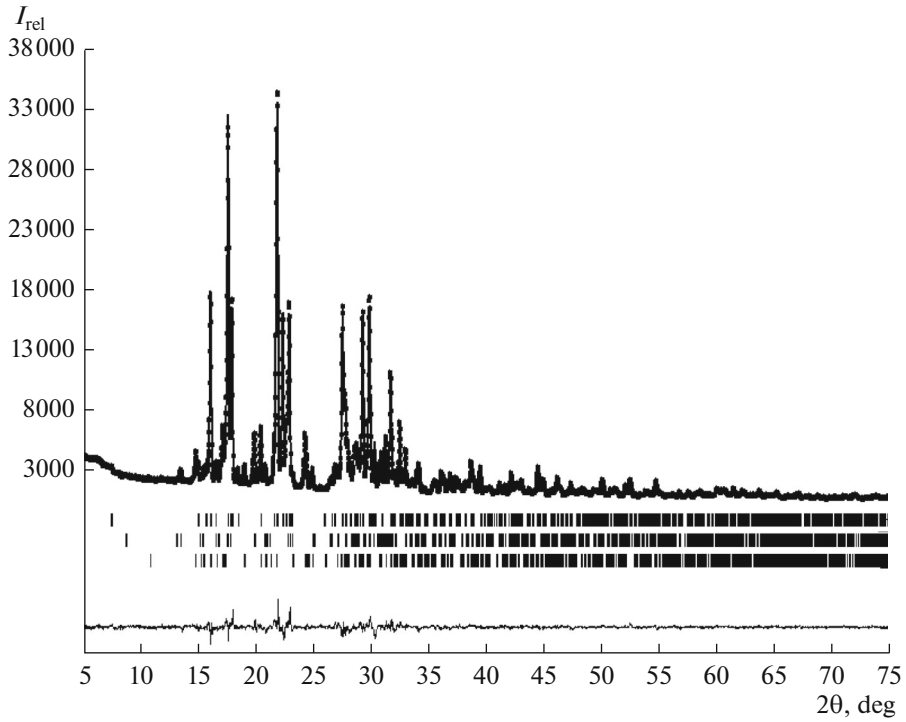

Fig. 5. Rietveld refinement for powder diffractogram of sample **III**. Dots show experimental curve, solid line displays calculation. Arrays of vertical dashes show diffraction maxima (upper row for **IIIa**, medium row for **IIIb**, lower row for **IIIc**). The lower curve displays the difference between experimental and calculated intensity values in each point.

The band at 1462 cm^{-1} may be assigned to mixed stretching deformational vibrations ν(CN) and δ(CNH). Deformational vibrations of CH_2 group provide the main contribution to the bands at 1440 and 1380 cm^{-1}. Medium intensity band at 1336 cm^{-1} and weak band at 1317 cm^{-1} correspond to asymmetrical and symmetrical ν(CN) vibrations, respectively.

The IR spectrum of compound **I** displays a strong band at 1111 cm^{-1} and very strong band at 1086 cm^{-1}, corresponding to vibrations $\nu_{as}(SO_4^{2-})$ and $\nu_s(SO_4^{2-})$, respectively. Such a high intensity of band at 1086 cm^{-1} (the strongest band in the all spectrum) seems to be due to the contribution of $\nu(CN^+)$ vibrations of the ethylenediamine fragment. Decrease in the symmetry

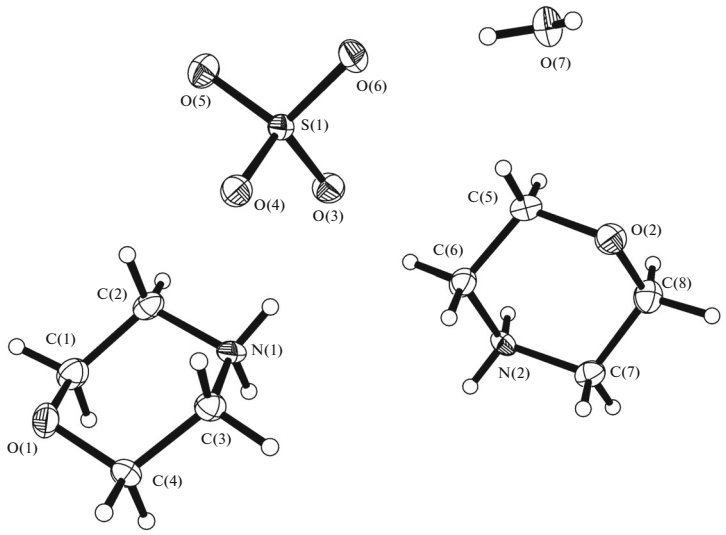

Fig. 6. Atom numbering scheme and thermal ellipsoids (probability level 50%) for structure **IV**. Letter A marks symmetrically equivalent atoms.

of SO_4^{2-} ion upon complexation is accompanied by the emergence in IR spectrum of strong band of fully symmetric stretching vibration $\nu_1(A_1)$ at 989 cm^{-1}. In similar manner, the strongest band in the spectrum of MP salt **IV** is a doublet at 1123 and 1105 cm^{-1} ($\nu_{as}(SO_4^{2-})$ and $\nu_s(SO_4^{2-}) + \nu(CN^+)$), while $\nu_1(A_1)$ is observed as a medium intensity band at 997 cm^{-1}. The strongest band in the spectrum of mixture of IIa and IIb is observed at 1122 cm^{-1}, which seems to be the superposition of $\nu_{as}(SO_4^{2-})$ and $\nu(CN^+)$ vibrations of ethylenediamine fragment. Vibration $\nu_1(A_1)$ for this complex appears as a strong band at 998 cm^{-1}.

The IR spectrum of the mixture of compounds **IIIa**, **IIIb**, and **IIIc** shows medium intensity bands at 1143 and 992 cm^{-1} corresponding to $\nu_{as}(SO_4^{2-})$ and $\nu_s(SO_4^{2-})$ vibrations, respectively. A shoulder at 503 cm^{-1} refers to $\delta_s(SO_4^{2-})$ deformational vibrations.

Three components of $\nu_4(SO_4^{2-})$ asymmetric deformational vibration appear in the IR spectrum of salt I as a strong doublet band with maxima at 639 and 609 cm^{-1} and medium intensity band at 672 cm^{-1}, whereas only one strong band at 619 cm^{-1} is observed in the spectra of TMEDA and MP salts.

Three bands in the region 510–440 cm^{-1} typical for the frequencies of symmetrical deformational vibrations of SO_4^{2-} ion refer to EDA salt. On can suppose that band at 464 cm^{-1} has a contribution of deformational vibrations $\delta(N^+–C–C–N^+)$ of the cation. Only medium intensity band at 518 cm^{-1} was revealed for the sample with TMEDA, while the spectrum of **IV** shows $\delta_s(SO_4^{2-})$, $\nu_{as}(SO_4^{2-})$ and $\nu_s(SO_4^{2-})$ bands similar to those of compound I.

Strong bands at 3013 and 2930 cm^{-1} in the spectrum of salt **I** correspond to stretching vibrations $\nu_{as}(NH_3^+)$ and $\nu_s(NH_3^+)$, respectively. Scissoring deformational vibrations of ammonium groups $\delta(H\overset{+}{N}H)$ and $\delta(C\overset{+}{N}H)$ are rather characteristic and appear as a doublet of strong bands at 1645 and 1631 cm^{-1}. Even stronger band at 1537 cm^{-1} seems to correspond to $\delta_s(NH_3^+)$. Bands in the region ~1560 cm^{-1} corresponding to deformational vibrations $\delta(NH_2^+)$ are present also in the spectra of complexes with piperazine and morpholine. This assignment is correct because of the lack of such a band in the spectrum of mixture of IIa with IIb where nitrogen in initial TMEDA is not hydrogenated. Bands in the region ~1635–1630 cm^{-1} are present in the spectra of all prepared compounds.

The spectra of onium salts of TMEDA and PP display bands in the region ~1210–1250 cm^{-1}, which can be assigned to $\nu_{as}(S_2O_6^{2-})$, and bands at ~580 cm^{-1} corresponding to $\delta(S_2O_6^{2-})$. This fact confirms that the obtained compounds includes dithionate ions along with sulfate (**IIa**, **IIIc**) and sulfite (**IIIa**) anions. Moreover, a band of $\nu_s(S_2O_6^{2-})$ at 1094 cm^{-1} is observed for PP sample.

We failed to perform correct identification of water absorption bands in IR spectra because of their overlapping with $\nu(NH)$ bands.

Table 3. Wave numbers (cm^{-1}) for the maxima of the main absorption bands in IR spectra for the products of SO_2 reaction with 1,2-diamines and morpholine

	I	IIa + IIb + IIc	IIIa + IIIb + IIIc	IV
$\nu_{as}(NH)$		3437 s br	3388 s	3418 s
$\nu_{s}(NH)$			3252 m	3286 s
$\nu_{as}(N^+H)$	3013 s	3019 s	3030 s	3035 s br
$\nu_{s}(N^+H)$	2930 s	2623 s	2616 w	2627 m
$\delta(HN^+H)$	1645 s			
$\delta(CN^+H)$	1631 s	1635 m br	1631 m	1634 m
$\delta_{as}(CNH)$			1492 w	
$\nu(CN) + \delta(CNH)$			1462 m	1464 w
$\delta_{s}(NH_3^+)$, $\delta(NH_2^+)$	1537 s		1560 w	1561 s
$\nu_{as}(CN)$			1335 m	
$\nu_{s}(CN)$			1317 w	1308 m, 1243 w, 1227 m
$\nu_{as}(S_2O_6^{2-})$		1240 m, 1214 w	1240 w, 1216 w	
$\nu_{s}(S_2O_6^{2-})$			1094 m	
$\nu_{as}(SO_4^{2-})$	1111 s		1143 m	1123 vs
$\nu_{as}(SO_4^{2-}) + \nu(CN^+)$	1086 vs	1122 vs	1105 m	1105 vs
$\nu_{as} + \nu_{s}(SO_3^{2-})$			1029 m, 1008 w, 992 w, 952 s, 905 s	
$\nu_{s}(SO_4^{2-})$	989 s	998 s	992 m	997 m
$\delta_{as}(SO_4^{2-})$	672 m, 639 s, 609 s	619 s	620 m	619 vs
$\delta_{s}(SO_3^{2-})$				
$\delta(S_2O_6^{2-})$		582 m	572 sh	
$\delta_{s}(SO_4^{2-})$	511 m, 442 m	518 m	503 sh	518 w, 438 s
$\delta_{d}(SO_3^{2-})$			492 m	
$\delta_{s}(SO_4^{2-}) + \delta(N^+–C–C–N^+)$	464 m		470 w	

It should be noted that PP under similar synthesis conditions [16] (reaction mixture pH PP : SO_2 = 3 : 2). A white onium sulfite was isolated in SO_2–EDA–Sol system (Sol is absolute ethanol, aqueous ethanol, or acetone) [17].

On the basis of above results, the data of our previous studies of SO_2–L–H_2O (L stands for alkylmonoamines) [18–21], and literature data, we can draw the following conclusion.

As shown in [22], sulfur(IV) oxide upon dissolution in water produces monohydrate (equation (1)), which dissociate to form hydrogen sulfite, pyrosulfite, and sulfite ions (equations (2)–(4)):

$$SO_2 + H_2O \rightarrow SO_2 \cdot H_2O, \quad (1)$$

$$SO_2 \cdot H_2O \overset{K_1}{\rightleftarrows} H^+ + HSO_3^-, \quad (2)$$

$$2HSO_3^- \overset{K}{\rightleftarrows} S_2O_5^{2-} + H_2O, \quad (3)$$

$$HSO_3^- \overset{K_2}{\rightleftarrows} H^+ + SO_3^{2-}. \quad (4)$$

According to the mechanism of free-radical oxidation of sulfite ion [23, 24], chain initiation proceeds due to decomposition of pyrosulfite ion:

$$S_2O_5^{2-} \rightleftarrows SO_3^{\bullet-} + SO_2^{\bullet-} \quad (5)$$

or via reaction of SO_3^{2-} ion with small amount of admixture metal ions of variable valence always present also in distilled water:

$$SO_3^{2-} + M^{n+} \rightleftarrows SO_3^{\bullet-} + M^{(n-1)+}. \quad (6)$$

Furthermore [25], SO_2 forms with organic nitrogen-containing bases (with MP, in particular) charge-transfer complexes, which also behave as sources of free radicals:

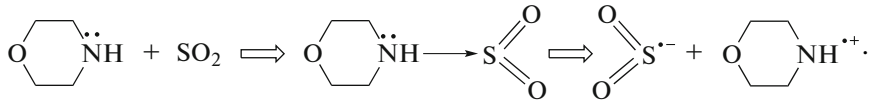
(7)

Chain propagation proceeds according to equations (8)–(15) [24]. In the systems producing onium dithionates, chain termination occurs by reaction (16). The lack of pyrosulfites in preparatively isolated products indicates the occurrence of reaction (17) [24]:

$$SO_3^{\bullet-} + O_2 \rightarrow SO_5^{\bullet-} \quad 2.5\times10^9, \quad (8)$$

$$SO_5^{\bullet-} + HSO_3^- \rightarrow HSO_5^- + SO_3^{\bullet-} \quad (3.4\text{–}8.6)\times10^2, \quad (9)$$

$$SO_5^{\bullet-} + HSO_3^- \rightarrow SO_4^{2-} + SO_4^{\bullet-} + H^+ \quad \le (2\text{–}3.6)\times10^2, \quad (10)$$

$$SO_5^{\bullet-} + SO_3^{2-} \rightarrow SO_5^{2-} + SO_3^{\bullet-} \quad 2.1\times10^5, \quad (11)$$

$$SO_5^{\bullet-} + SO_3^{2-} \rightarrow SO_4^{2-} + SO_4^{\bullet-} \quad 5.5\times10^5, \quad (12)$$

$$SO_4^{\bullet-} + HSO_3^- \rightarrow SO_4^{2-} + SO_3^{\bullet-} + H^+ \quad (6.8\text{–}7.5)\times10^8, \quad (13)$$

$$SO_4^{\bullet-} + SO_3^{2-} \rightarrow SO_4^{2-} + SO_3^{\bullet-} \quad (3.1\text{–}5.7)\times10^8, \quad (14)$$

$$SO_5^{\bullet-} + SO_5^{\bullet-} \rightarrow SO_4^{\bullet-} + SO_4^{\bullet-} + O_2 \quad (8.7\text{–}22)\times10^7, \quad (15)$$

$$SO_3^{\bullet-} + SO_3^{\bullet-} \rightarrow S_2O_6^{2-}, \quad (16)$$

$$HSO_5^- + HSO_3^- + H^+ \rightarrow 2SO_4^{2-} + 3H^+ \quad \approx10^7[H^+]. \quad (17)$$

The isolation of sulfates **I**, **IIa**, **IIIc**, and **IV**, as well as the results [18–21], indicates the presence of reactions (10), (13), (14), and (17); the isolation of dithionates **IIb** and **IIIb** as mixtures evidences the occurrence of reaction (16).

We previously [27–30] isolated onium sulfites from SO_2–L–H_2O systems (L is ethanolamine, aminoguanidine) under similar conditions because alkanols inhibit sulfooxidation [31–33]. In the case of TRIS, onium sulfate forms under similar conditions [19]. In contrast to the results [27], diethanolamine accelerates S(IV) oxidation, while triethanolamine is inert [34].

The established fact that EDA and MEA additives partially suppress the catalytic oxidation of sodium sulfite under the action of 3*d* metal cations (Mn^{2+}, Fe^{2+}, and Cu^{2+}) [32] seems to indicate that the formation of free radicals via reaction (6) in the studies systems is unlikely.

The possibility to realize the process of mild SO_2 oxidation under reported synthesis conditions using a wider series of amine ligands will be elucidated in further studies.

REFERENCES

1. K. Eller, E. Henkes, R. Rossbacher, and H. Hoke, *Ullmann's Encyclopedia of Industrial Chemistry* (Wiley-VCH, Weinheim, 2005), Vol. 2, p. 647. doi 10.1002/14356007.a02_001
2. K. Jayaraman, A. Choudhury, and C. N. R. Rao, Solid State Sci. **4**, 413 (2002). doi 10.1016/S1293-2558(02)01269-4
3. L. A. Cuccia, L. Koby, J. B. Ningappa, and M. Dakessian, J. Chem. Educ. **82**, 1043 (2005). doi 10.1021/ed082p1043
4. N. C. Santhakumari and C. P. G. Vallabhan, J. Phys. Chem. Solids **53**, 697 (1992). doi 10.1016/0022-3697(92)90210-5
5. J. Bellanato, Spectrochim. Acta **16**, 1344 (1960). doi 10.1016/S0371-1951(60)80008-2
6. M. K. Marchewka and M. Drozd, Spectrochim. Acta, Part A Mol. Biomol. Spectrosc. **99**, 223 (2012). doi 10.1016/j.saa.2012.09.026
7. B. R. Srinivasan, S. S. Khandolkar, R. N. Jyai, et al., Spectrochim. Acta, Part A Mol. Biomol. Spectrosc. **102**, 235 (2013). doi 10.1016/j.saa.2012.09.103
8. B. M. Yamin, L. Narimani, and N. Ibrahim, Int. J. Adv. Sci., Eng. Inf. Technol. **3** (2), 47 (2013).
9. V. A. Klimova, *The Main Methods for Analysis of Organic Compounds* (Khimiya, Moscow, 1975) [in Russian].
10. G. M. Sheldrick, Acta Crystallogr., Sect. A: Found. Crystallogr. **64**, 112 (2008). doi 10.1107/S0108767307043930
11. N. S. Vul'fson, V. G. Zaikin, and A. I. Mikaya, *Mass Spectrometry of Organic Compounds* (Khimiya, Moscow, 1986).
12. T. Guerfel, A. Gharbi, and A. Jouini, J. Soc. Alger. Chim. **2**, 125 (2007).
13. S. Gunasekaran and B. Anita, Ind. J. Pure Appl. Phys. **46**, 833 (2008).

14. R. A. Nyquist and R. O. Kagel, *Handbook of Infrared and Raman Spectra of Inorganic Compounds and Organic Salts* (Academic, New York, 1996), Vol. 4.
15. K. Nakamoto, *Infrared and Raman Spectra of Inorganic and Coordination Compounds* (Interscience, New York, 1986).
16. US Patent No. 3046277 (1962).
17. US Patent No. 2069165 (1937).
18. R. E. Khoma, A. A. Ennan, O. V. Shishkin, et al., Russ. J. Inorg. Chem. **57**, 1559 (2012). doi 10.1134/S003602361212008X
19. R. E. Khoma, V. O. Gel'mbol'dt, O. V. Shishkin, et al., Russ. J. Inorg. Chem. **59**, 1 (2014). doi 10.1134/S0036023614010069
20. R. E. Khoma, A. A. Ennan, V. O. Gelmboldt, et al., Russ. J. Gen. Chem. **84**, 637 (2014). doi 10.1134/S1070363214040069
21. R. E. Khoma, V. O. Gel'mbol'dt, V. N. Baumer, et al., Russ. J. Inorg. Chem. **60**, 1199 (2015). doi 10.1134/S0036023615100101
22. S. Pereda, K. Thomsen, and P. Rasmussen, Chem. Eng. Sci. **55**, 2663 (2000). doi 10.1016/S0009-2509(99)00535-7
23. S. K. Fedorova, I. P. Skibida, and A. V. Gladkii, Zh. Prikl. Khim. **50**, 716 (1976).
24. A. N. Ermakov and A. P. Purmal', Kinet. Catal. **42**, 479 (2001). doi 10.1023/A:1010565304435
25. P. Ghosh and G. Pal, J. Polym. Sci., Part A: Polym. Chem. **36**, 1973 (1998). doi 10.1002/(SICI)1099-0518(19980915)36:12<1973::AID-POLA1>3.0.CO;2-P
26. G. Qing-yu, L. Run-ming, Y. Geng-xu, et al., Imag. Sci. Photochem. **19**, 116 (2001). doi 10.7517/j.issn.1674-0475.2001.02.116
27. R. E. Khoma, V. O. Gel'mbol'dt, L. V. Koroeva, et al., Vopr. Khim. Khim. Tekhnol., No. 1, 133 (2012).
28. R. E. Khoma, A. A. Ennan, A. V. Mazepa, and V. O. Gel'mbol'dt, Vopr. Khim. Khim. Tekhnol., No. 1, 136 (2013).
29. R. E. Khoma, V. O. Gelmboldt, O. V. Shishkin, et al., Russ. J. Inorg. Chem. **84**, 541 (2014). doi 10.1134/S0036023614060096
30. R. E. Khoma, V. O. Gelmboldt, V. N. Baumer, et al., Russ. J. Inorg. Chem. **58**, 843 (2013). DOI: doi 10.1134/S0036023613070140
31. U. Deister and P. Warnek, J. Phys. Chem. **94**, 2191 (1990). doi 10.1021/j100368a084
32. J. Ziajka and W. Pasiuk-Bronikowska, Atmos. Environ. **37**, 3913 (2003). doi 10.3109/10715769309056520
33. US Patent No. 213032 (1938).
34. US Patent No. 4310438 (1982).

Translated by I. Kudryavtsev